

Early-Outgrowth Bone Marrow Cells Attenuate Renal Injury and Dysfunction via an Antioxidant Effect in a Mouse Model of Type 2 Diabetes

Yanling Zhang, Darren A. Yuen, Andrew Advani, Kerri Thai, Suzanne L. Advani, David Kepecs, M. Golam Kabir, Kim A. Connelly, and Richard E. Gilbert

Cell therapy has been extensively investigated in heart disease but less so in the kidney. We considered whether cell therapy also might be useful in diabetic kidney disease. Cognizant of the likely need for autologous cell therapy in humans, we sought to assess the efficacy of donor cells derived from both healthy and diabetic animals. Eight-week-old db/db mice were randomized to receive a single intravenous injection of PBS or 0.5×10^6 early-outgrowth cells (EOCs) from db/m or db/db mice. Effects were assessed 4 weeks after cell infusion. Untreated db/db mice developed mesangial matrix expansion and tubular epithelial cell apoptosis in association with increased reactive oxygen species (ROS) and overexpression of thioredoxin interacting protein (TxnIP). Without affecting blood glucose or blood pressure, EOCs not only attenuated mesangial and peritubular matrix expansion, as well as tubular apoptosis, but also diminished ROS and TxnIP overexpression in the kidney of db/db mice. EOCs derived from both diabetic db/db and nondiabetic db/m mice were equally effective in ameliorating kidney injury and oxidative stress. The similarly beneficial effects of cells from healthy and diabetic donors highlight the potential of autologous cell therapy in the related clinical setting. *Diabetes* 61:2114–2125, 2012

The discovery that certain bone marrow–derived cells can assist in tissue repair has led to a broad range of preclinical and human studies focusing in particular on the potential of these cells as a new therapeutic strategy in cardiovascular disease (1). Although the mechanism(s) whereby they exert their beneficial effect remains uncertain, several studies have documented only minimal retention of administered cells within organs that have nevertheless sustained functional and structural improvements (2–4). Appreciation of these findings has, accordingly, led to the assertion that certain types of bone marrow–derived cells may affect tissue repair by the secretion of locally active paracrine factors rather than by their incorporation into pre-existing structures (4–6). Particularly prominent with regard to their secretory output are the so-called early-outgrowth cells (EOCs), defined more by the culture techniques used to grow them than by their cell surface markers (7). Although most studies have focused on the proangiogenic activity of bone marrow cells, EOCs have been shown to secrete

factors with antifibrotic actions (8) and most recently to also elaborate soluble factors that protect mature endothelial cells from oxidative stress, attenuating H_2O_2 -induced apoptosis (9).

The excessive production of reactive oxygen species (ROS) has been implicated in a wide range of common degenerative disorders, such as atherosclerosis, Alzheimer's disease, ageing, and, in particular, diabetes, where the excessive superoxide production, arising from increased glycolytic flux, provides a cogent explanation for the long-term complications of the disease (10), especially nephropathy (11). However, in addition to enhancing ROS production, hyperglycemia also may lead to dysregulation of the antioxidant defenses that remove ROS and repair oxidized molecules. In particular, diabetes leads to a dramatic diminution in the activity of the major thiol-reducing thioredoxin (Trx) system as a consequence of the overexpression of its endogenous inhibitor, Trx inhibitory protein (*TxnIP*) (12–17).

In light of the role of ROS in the pathogenesis of diabetic nephropathy and the ability of EOCs to protect cells from H_2O_2 -induced injury (9), we considered whether such cells may also diminish high glucose–induced oxidative stress and protect the kidney from the damaging effects of the diabetic milieu. Moreover, given the importance of high glucose–induced *TxnIP* overexpression in attenuating the cell's ability to remove ROS, we further sought to determine whether EOCs might dampen this paradoxical and deleterious response to the diabetic milieu.

Here we show that a single intravenous infusion of EOCs not only attenuated diabetes-induced ROS and *TxnIP* overexpression in the diabetic kidney but did so in association with reduced matrix expansion, fewer apoptotic cells, and a curtailment in the rise of albuminuria. Indeed, not only was EOC infusion able to attenuate the excess ROS and TxnIP overexpression in vivo but the cell-free culture medium in which the EOCs had been grown was similarly effective in the in vitro setting.

RESEARCH DESIGN AND METHODS

Animal model and experimental design. Thirty-six 6-week-old male diabetic db/db (*BKS.Cg-Dock7 m^{+/+} Leprdb/J*) and 12 age-matched db/m (*Dock7 m^{+/+} Leprdb*; heterozygote from the same colony) mice were purchased from The Jackson Laboratory (Bar Harbor, ME). At 8 weeks of age, the db/db mice were randomized to receive a tail vein injection of 1) Dulbecco's PBS (DPBS; $n = 12$), 2) 5×10^5 EOCs derived from db/m mice ($n = 12$), or 3) 5×10^5 EOCs derived from db/db mice. Db/m mice served as nondiabetic controls. Mice were housed in a temperature-controlled room (22°C) with a 12-h:12-h light:dark cycle with free access to food and water. All animal studies were approved by the St. Michael's Hospital Animal Ethics Committee in accordance with the *Guide for the Care and Use of Laboratory Animals* (NIH publ. no. 85-23, revised 1996). Four weeks after treatment, the animals were killed, urine and blood samples were collected, and kidney tissues were harvested.

From the Keenan Research Centre of the Li Ka Shing Knowledge Institute, St. Michael's Hospital, University of Toronto, Toronto, Ontario, Canada. Corresponding author: Richard E. Gilbert, richard.gilbert@utoronto.ca. Received 11 October 2011 and accepted 10 March 2012.

DOI: 10.2337/db11-1365

Y.Z. and D.A.Y. contributed equally to this work.

© 2012 by the American Diabetes Association. Readers may use this article as long as the work is properly cited, the use is educational and not for profit, and the work is not altered. See <http://creativecommons.org/licenses/by-nc-nd/3.0/> for details.

Bone marrow harvesting and cell culture. EOCs were cultured as previously described (8). In brief, bone marrow cells were collected from the femora and tibiae of 3- to 4-week-old male db/m or db/db mice and cultured in endothelial growth medium-2 (EGM-2; Lonza, Walkersville, MD) at 37°C with 5% CO₂ for 7–10 days to produce EOCs.

Cell infusion. EOCs were washed with DPBS to remove all medium components. Viable cells were analyzed by trypan blue exclusion and counted by a hemocytometer. Cells were resuspended in DPBS at a final concentration of 2×10^6 EOCs/mL. Eight-week-old db/db mice received an infusion of 5×10^5 db/m EOCs, 5×10^5 db/db EOCs, or DPBS by tail vein injection.

Renal and metabolic functional parameters. Body weight and blood glucose (Accu-Check Advantage; Roche, Mississauga, ON) were determined biweekly. Urinary albumin excretion was determined after 24 h of metabolic caging at baseline and study end with an AssayMax mouse albumin ELISA (Assaypro, St. Charles, MO). At the end of the study, invasive blood pressure was measured in anesthetized mice (2% isoflurane) using a Millar instrument (model SPR-838; Houston, TX), and systolic blood pressure was calculated with Millar analysis software PVAN 3.4.

Renal histology. Four-micrometer sections were used for periodic acid-Schiff (PAS) staining or immunostaining. Frozen tissues embedded in cryostat matrix were cut into 30- μ m sections prior to staining and confocal microscopic analysis. Mesangial expansion was assessed as described previously (18). Immunohistochemistry was performed as previously described (19). Stained sections were scanned with the Aperio Ultra-Resolution Digital Scanning System (Aperio Technologies, Vista, CA), with the acquired images analyzed using Aperio ImageScope software. Type IV collagen deposition was quantified in 30 randomly selected glomeruli and 15 random, nonoverlapping 20 \times fields for each animal in a masked fashion.

Terminal deoxynucleotidyl transferase-mediated dUTP nick-end labeling. Renal cell apoptosis was assessed using terminal deoxynucleotidyl transferase-mediated dUTP nick-end labeling (TUNEL). TUNEL-positive cells were counted in 50 randomly selected glomeruli and in 15 random, nonoverlapping 20- μ m fields in the cortical tubulointerstitium for each kidney section.

Renal oxidative stress. Superoxide ion generation was assessed by quantifying the conversion of dihydroethidium to ethidium, as previously described (20). Images were obtained with a Leica TCS SL confocal microscope. Fluorescence was detected with a 585-nm long-pass filter. Laser settings were identical for acquisition of images from all specimens.

5-(and-6)-4-Chloromethyl-benzoyl-amino-tetramethylrhodamine labeling and EOC tracking. Cultured EOCs from db/m mice were labeled with a 5 μ mol/L solution of 5-(and-6)-4-chloromethyl-benzoyl-amino-tetramethylrhodamine (CMTMR; Invitrogen), as previously described (8). One-half million CMTMR-labeled EOCs were then infused via tail vein injection into 8-week-old db/db mice. Animals were killed at 1, 4, 7, 14, and 28 days after cell infusion. One-half million CMTMR-labeled cultured fibroblasts from db/m mice were similarly infused to provide a cell-based control, in addition to PBS administration. The presence of CMTMR-positive cells in kidney, liver, lung, and spleen was determined on a confocal laser-scanning microscope by counting CMTMR-positive cells in 10 randomly selected 40 \times fields per section. CMTMR-positive cells in the bone marrow were quantified and expressed as a percentage of all bone marrow cells.

In vitro studies. Normal rat kidney (NRK) cells were cultured as previously described (16). Cells were subjected to five culture conditions: 1) DMEM with 5.6 mmol/L glucose (NG), 2) DMEM with 25 mmol/L glucose (HG), 3) DMEM with 10% 10-times concentrated db/m EOC-conditioned medium and 25 mmol/L glucose (HG + db/m CM), 4) DMEM with 10% 10-times concentrated db/db EOC-conditioned medium and 25 mmol/L glucose (HG + db/db CM), or 5) mannitol (25 mmol/L) added to DMEM as an osmotic control. After culturing in these conditions for 48 h, cells were subjected to studies of intracellular ROS levels and *Trx/TxnIP* gene expression. EOC-conditioned medium was generated as previously described (8). Endothelial cell basal medium-2 (Lonza) was used to generate EOC-conditioned medium and served as a negative control for the in vitro studies.

EOC cell surface markers. To assist in determining their identity, cell surface markers were examined in both freshly isolated bone marrow and EOCs by flow cytometry (FACSCalibur) using CellQuest data acquisition and analysis software. FITC-CD34, PE-VEGFR2, APC Cy7 CD11b, and FITC-Ly6C antibodies were purchased from BD Biosciences, and PE-CD133 antibody was obtained from Biogen. Cells incubated with conjugated irrelevant IgGs were used as negative controls.

Intracellular ROS levels. After 48 h of exposure to the described experimental conditions, NRK tubular cells were stained with 5-(and 6)-chloromethyl-2',7'-dichlorodihydrofluorescein diacetate, acetyl ester (CM-H2-DCFDA; Invitrogen), as previously described (16). The intracellular ROS was determined by measuring 10,000 events per sample following excitation with a 488-nm wavelength laser and reading through a 525/50 filter using a flow cytometer (FACSCalibur). Flow cytometry data were analyzed using WinMDI 2.9 (Scripps Institute, La Jolla, CA).

Real-time quantitative RT-PCR. Real-time quantitative PCR was used to determine the relative expression levels of *Trx* and *TxnIP* transcripts as described previously (16). Primers were obtained from Sigma-Aldrich. Primer sequences were as follows: *mRPL13a* forward GCT CTC AAG GTT GTT CGG CTG A and reverse AGA TCT GCT TCT TCC GAT A; mouse *TxnIP* forward TCA AGG GCC CCT GGG AAC ATC C and reverse GAC ACT GGT GCC ATT AAG TCA G; and mouse *Trx* forward CAA ATG CAT GCC GAC CTT CCA GTT and reverse TGG CAG TTG GGT ATA GAC TCT CCA. Experiments were performed in triplicate, and data analyses were performed using the Applied Biosystems Comparative CT method. All values were referenced to the mRNA transcript levels of the housekeeper gene Rpl13a. To assess factors responsible for ROS production, we also examined NADPH Oxidase 4 (*Nox-4*), catalase, Cu/Zn superoxide dismutase (*Cu/Zn SOD*) and Mn superoxide dismutase (*Mn SOD*) expression by real-time quantitative PCR using primers and reagents from Applied Biosystems (assay IDs: Mm00479246.m1).

Cytokine array. The breadth of EOC cytokine expression was examined by protein array (Proteome Profiler Cytokine Array kit; R&D Systems, Minneapolis, MN), according to the manufacturer's instructions. Cytokine expression was quantified densitometrically using ImageJ software (National Institutes of Health, Bethesda, MD).

Statistical analysis. All data are shown as means \pm SEM, unless otherwise stated. Differences between groups were analyzed by ANOVA and unpaired Student *t* tests for two group comparisons. Post hoc differences between subgroups were analyzed using the Fisher least significant differences test. All statistics were performed using GraphPad Prism 4.00 for Windows (GraphPad Software, San Diego, CA) or SPSS 15.0 for Windows (SPSS, Chicago, IL). A change was considered statistically significant if $P < 0.05$.

RESULTS

Animal characteristics. The characteristics of the db/m and db/db mice with and without EOC infusion are presented in Table 1. In comparison with db/m mice, db/db mice developed hyperglycemia and increased body weight that were unaffected by EOC infusion. All four groups had normal systolic blood pressure that was similarly unaffected by EOC administration. As expected, db/db mice had considerably greater albuminuria when compared with db/m mice at 8 weeks of age, the time at which they were randomized to receive either cells or PBS. Over the ensuing 4 weeks, albuminuria increased further, approximately doubling in db/db mice that received PBS (108 ± 4 vs. 215 ± 8 mg/day, 8 vs. 12 weeks, $P < 0.05$). In contrast, diabetic mice that had received EOCs from either db/m

TABLE 1
Animal characteristics

Characteristic	db/m	db/db + PBS	db/db + db/m EOC	db/db + db/db EOC
Blood glucose (mmol/L)	6.5 \pm 0.1	26.7 \pm 0.6*	27.7 \pm 0.7*	30.4 \pm 0.4*
Systolic blood pressure (mmHg)	104.9 \pm 1.4	104.6 \pm 0.8	109.9 \pm 1.9	107.8 \pm 1.7
Body weight (g)	27.7 \pm 0.2	44.3 \pm 0.7*	45.9 \pm 0.8*	41.7 \pm 0.3*
Kidney weight (g)	0.33 \pm 0.01	0.37 \pm 0.01*	0.37 \pm 0.01*	0.36 \pm 0.01*
Kidney weight/body weight	1.22 \pm 0.03	0.83 \pm 0.02*	0.82 \pm 0.01*	0.88 \pm 0.01*

* $P < 0.05$ vs. db/m group.

or db/db donor mice showed no significant progression (157 ± 5 vs. 104 ± 5 mg/day for db/db EOC recipients, 8 vs. 12 weeks, $P = \text{NS}$; 140 ± 6 vs. 185 ± 9 mg/day for db/m EOC recipients, $P = \text{NS}$).

Cell surface markers. To further determine the attributes of the EOCs, we examined their cell surface markers by fluorescence-activated cell sorter analysis. Among freshly isolated nucleated bone marrow cells, 65% were Ly6C^+ , 20% CD11b^+ , 6% CD34^+ , 7% CD133^+ , and 3% VEGFR^+ (Fig. 1A–H). In contrast, virtually all EOCs were CD34^+ and VEGFR^+ , albeit weakly so. No cell surface expression of either CD133 or the monocyte marker CD11b was noted among EOCs, and although the vast majority of cells were

Ly6C^- , a small proportion (0.42%) was strongly positive for this cell surface marker (Fig. 1I–P).

Histopathology. When compared with their nondiabetic, db/m counterparts, PAS-stained kidneys of db/db mice displayed prominent mesangial expansion and glomerular hypertrophy, which was ameliorated although not entirely normalized by EOC administration (Fig. 2A–F). Collagen type IV immunolabeling was localized to the glomerular mesangium. When compared with nondiabetic db/m mice, the kidneys of diabetic db/db animals demonstrated substantially increased abundance of immunostainable collagen IV in mesangial areas. Treatment with EOCs from either db/m or db/db donor mice attenuated these changes (Fig. 2G–K).

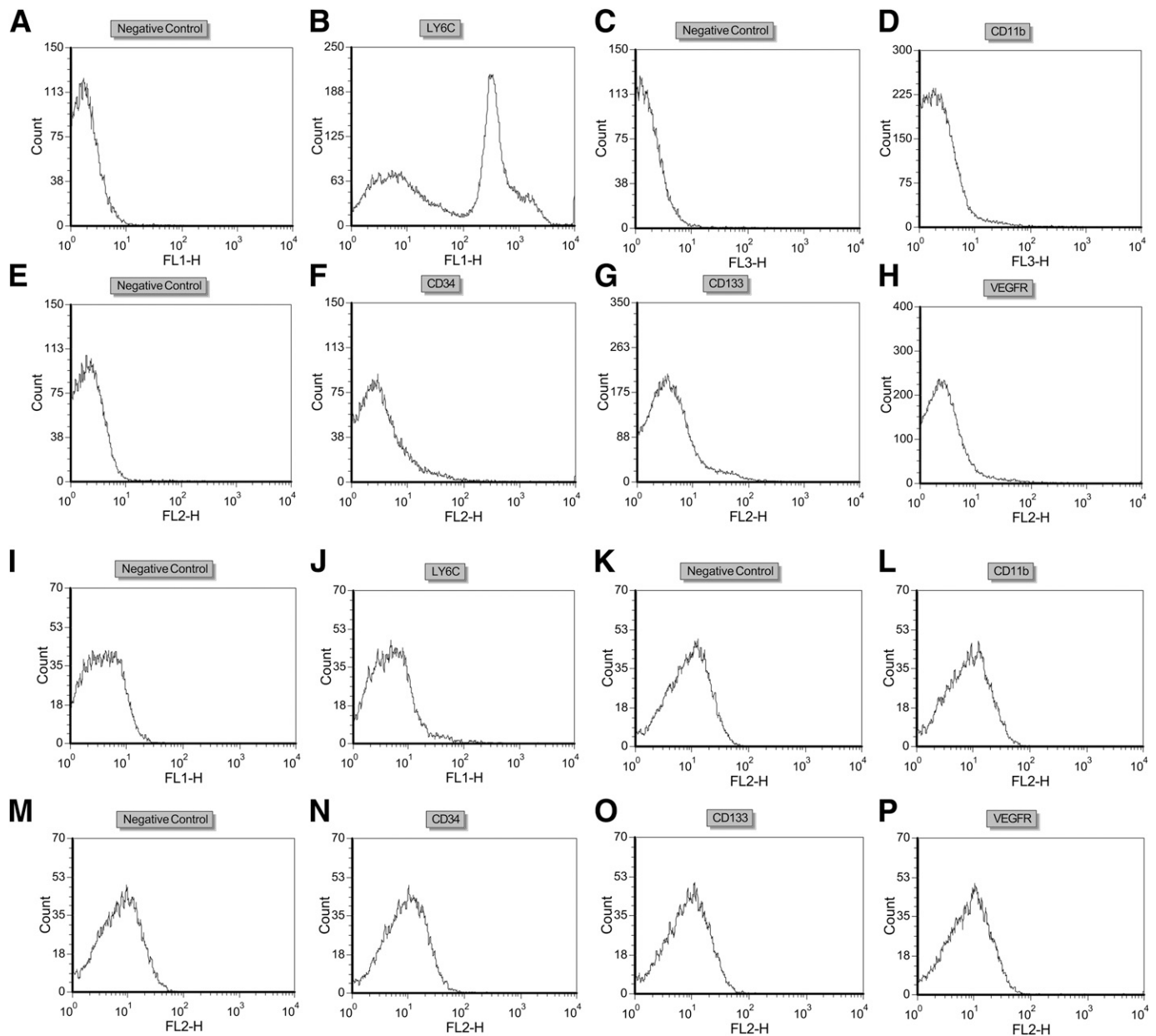


FIG. 1. Cell surface markers. Cell surface markers were examined by flow cytometry in freshly isolated nucleated bone marrow cells (A–H) and cultured EOCs (I–P). Freshly isolated nucleated bone marrow cells were mostly Ly6C^+ (65%) with other cell surface markers present on a smaller proportion of cells (20% CD11b^+ , 6% CD34^+ , 7% CD133^+ , and 3% VEGFR^+). Almost all EOCs were weakly CD34^+ and VEGFR^+ . A small proportion of EOCs (0.42%) was strongly positive for Ly6C . Negative control for Ly6C (A and I); Ly6C (B and J); negative control for CD11b (C and K); CD11b (D and L); negative control for CD34 , CD133 , and VEGFR (E and M); CD34 (F and N); CD133 (G and O); and VEGFR (H and P). Cells incubated with conjugated irrelevant IgGs were used as negative controls.

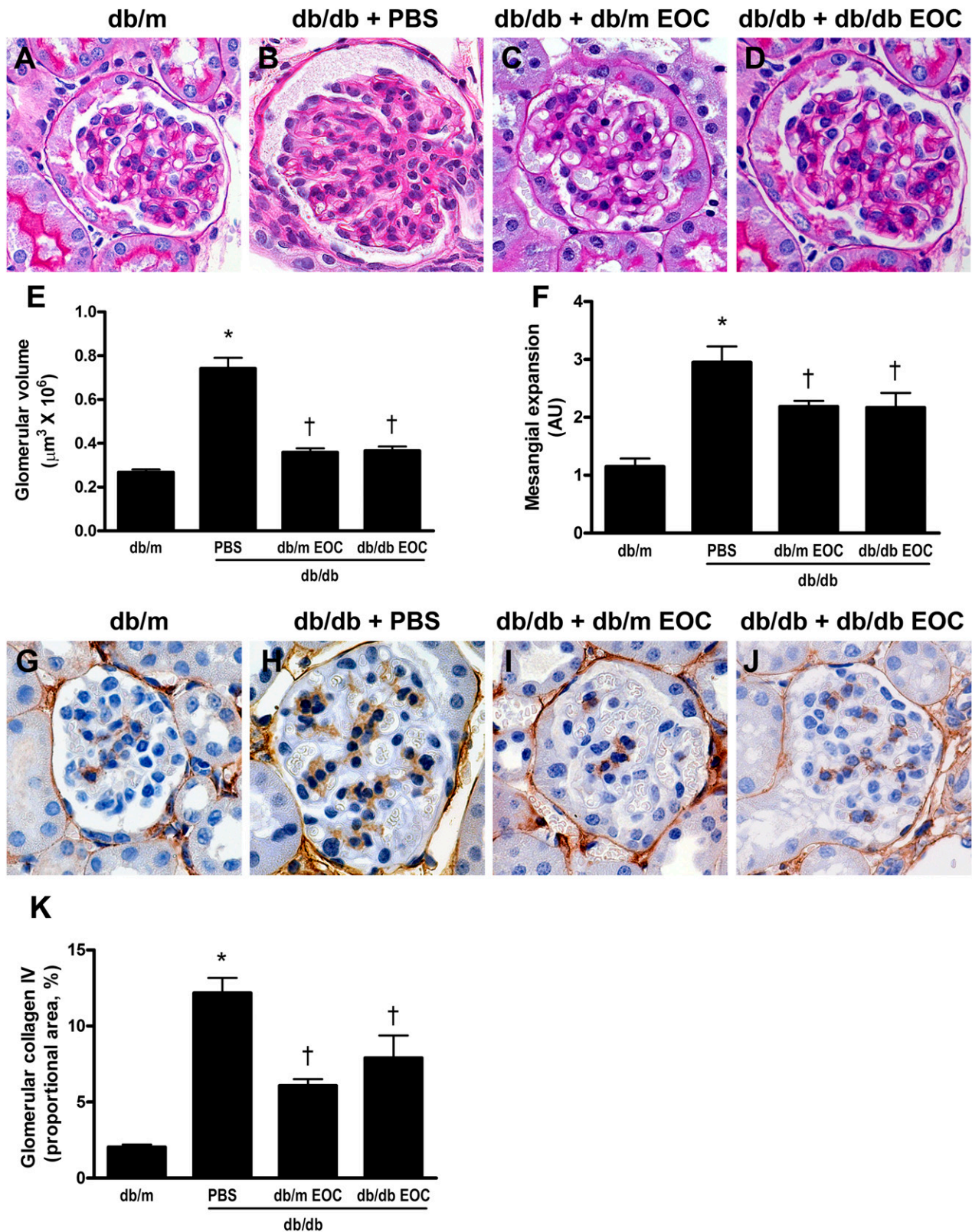


FIG. 2. Glomerular pathology is ameliorated by EOC administration. Kidney sections were stained with PAS (A–D) or immunolabeled with anti-collagen type IV antibody (G–J). Representative photomicrographs from db/m mice (A and G), PBS-treated db/db mice (B and H), db/m EOC-treated db/db mice (C and I), and db/db EOC-treated db/db mice (D and J) are shown along with graphs displaying the magnitude of glomerular volume (E), mesangial expansion (F), and glomerular collagen IV immunostaining (K). Original magnification: $\times 400$. * $P < 0.05$ vs. db/m animals; † $P < 0.05$ vs. PBS-treated db/db animals. (A high-quality digital representation of this figure is available in the online issue.)

Peritubular matrix expansion and tubular epithelial cell apoptosis are attenuated by EOC administration.

At 12 weeks of age, when compared with db/m mice, the kidneys of db/db mice demonstrated significantly increased collagen IV accumulation in peritubular regions, which was reduced in the kidneys of both db/m EOC- and db/db EOC-treated animals (Fig. 3A–D and I). TUNEL-positive apoptotic cells were only rarely seen in db/m mouse kidneys (Fig. 3E). In contrast, numerous TUNEL-positive cells were readily apparent within the tubules of db/db mice (Fig. 3F). Diabetic db/db mice that had received EOCs from either db/m or db/db donor mice, however, showed a marked reduction in the extent of TUNEL labeling in their tubules (Fig. 3G and H). Quantification of apoptotic cells in tubules is shown in Fig. 3J. Apoptotic cells were not present in glomeruli of either db/db or db/m mice.

EOCs reduce superoxide generation in the diabetic kidney. Kidney sections, labeled with dihydroethidium, which produces a red fluorescence when oxidized to ethidium in the presence of O_2^- , demonstrated an approximately threefold increase in fluorescence within the cortical tubules and glomeruli of db/db mice when compared with nondiabetic db/m animals ($P < 0.05$). These diabetes-related changes were substantially diminished in animals that had received EOCs from either db/m or db/db donor mice (Fig. 4A–J).

Renal expression of Trx and TxnIP. To investigate the mechanisms underlying the increased oxidative stress observed in the kidney of db/db mice, we examined the expression of *Trx* and *TxnIP* along with other enzymes that modulate ROS. *TxnIP* mRNA was 6.5-fold higher in untreated diabetic db/db mice than in db/m controls ($P < 0.05$). EOC infusion from either db/m or db/db donor mice

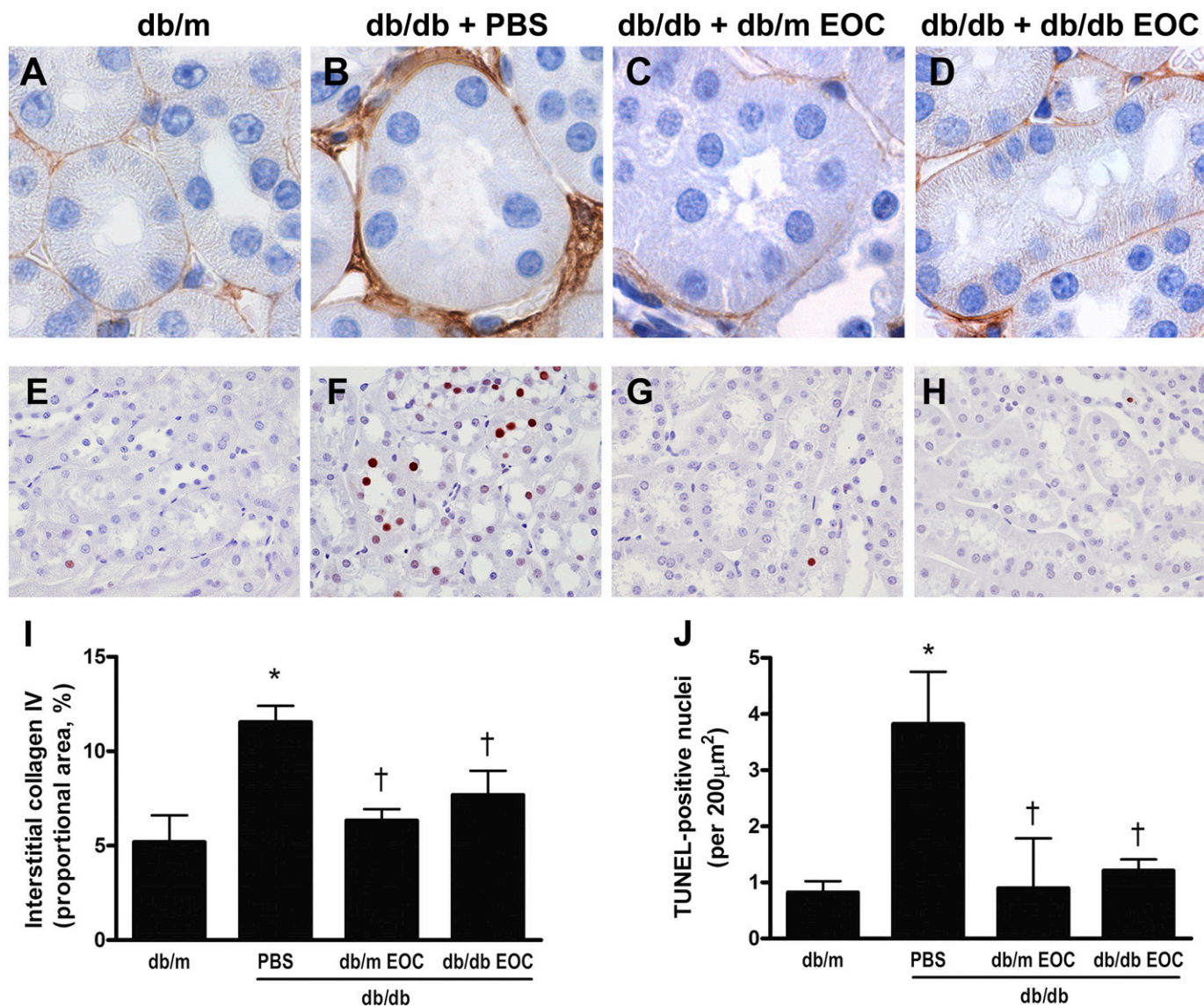


FIG. 3. Peritubular matrix expansion and tubular epithelial cell apoptosis were attenuated by EOC treatment. Collagen type IV deposition was examined by immunochemistry (A–D) and tubular epithelial cell apoptosis was assessed by TUNEL (E–H). Representative photomicrographs from db/m mice (A and E), PBS-treated db/db mice (B and F), db/m EOC-treated db/db mice (C and G), and db/db EOC-treated db/db mice (D and H) are shown along with graphs displaying the magnitude of peritubular collagen IV immunostaining (I) and TUNEL-positive nuclei (J). Original magnification: $\times 400$ (A–D); $\times 160$ (E–H). * $P < 0.05$ vs. db/m animals; † $P < 0.05$ vs. PBS-treated db/db animals. (A high-quality digital representation of this figure is available in the online issue.)

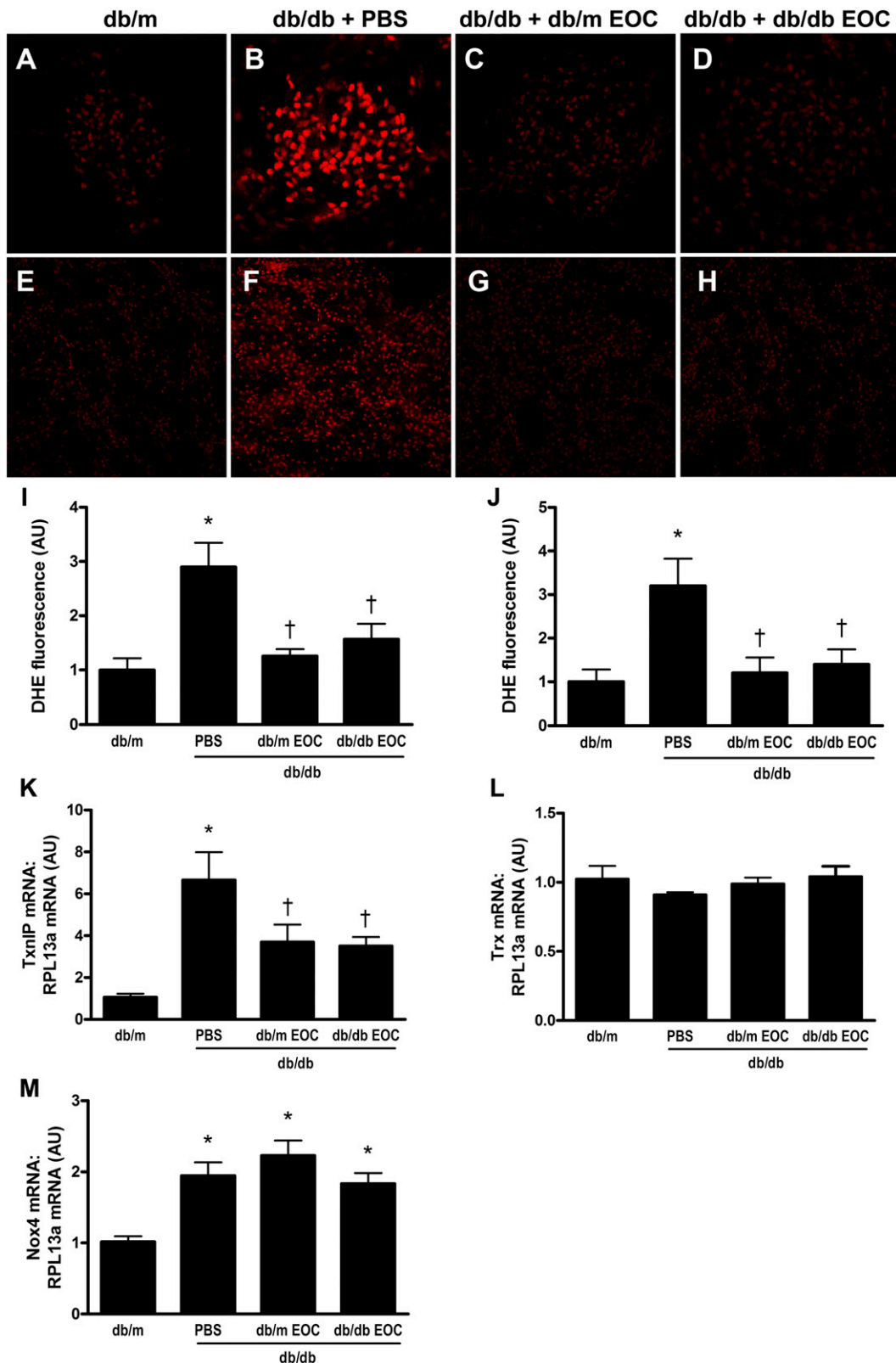


FIG. 4. EOC treatment reduces oxidative stress and *TxnIP* overexpression in the kidney of *db/db* mice. Representative photomicrographs showing ethidium fluorescence (red) in glomeruli and tubulointerstitium of *db/m* mice (*A* and *E*), PBS-treated *db/db* mice (*B* and *F*), *db/m* EOC-treated *db/db* mice (*C* and *G*), and *db/db* EOC-treated *db/db* mice (*D* and *H*). *I* and *J*: Quantification of ethidium fluorescence in glomeruli and tubulointerstitial area also are shown. EOC-induced reduction in ethidium fluorescence was accompanied by attenuation in the overexpression of *TxnIP* in the kidneys of EOC-treated *db/db* mice (*K*), as assessed by quantitative RT-PCR. *L*: Renal *Trx* mRNA was similar in all four groups. *M*: *Nox-4* mRNA was elevated in the kidneys of *db/db* mice and was unaffected by EOC treatment. Ethidium fluorescence and mRNA levels of *TxnIP*, *Trx*, and *Nox-4* were all expressed relative to *db/m* mice levels (that were arbitrarily assigned a value of 1). DHE, dihydroethidium; original magnification in glomeruli: $\times 400$ (*A–D*); in tubulointerstitial areas $\times 40$ (*E–H*). * $P < 0.05$ vs. *db/m* animals; † $P < 0.05$ vs. PBS-treated *db/db* animals. (A high-quality digital representation of this figure is available in the online issue.)

reduced the magnitude of *TxnIP* mRNA overexpression to a similar extent (Fig. 4K). Renal *Trx* expression, on the other hand, was similar in all four groups, and although *Nox-4* expression was increased twofold in db/db mice kidneys, it was unaffected by EOC treatment (Fig. 4L and M). No difference in catalase, *Cu/Zn SOD*, or *MnSOD* expression in the kidneys between the groups was noted (data not shown).

Administered EOCs are not retained in the kidney. EOCs that had been labeled with the fluorescent marker, CMTMR, were notably absent from the kidneys of db/db

mice at both early and later time points after EOC infusion. In contrast, abundant labeled cells were present in the liver, spleen, bone marrow, and lung, persisting in all but the latter during the 4 weeks of study (Fig. 5). However, no CMTMR-labeled fibroblasts were detected in any of these organs 4 weeks following their infusion.

EOC-conditioned medium attenuates oxidative stress in cultured proximal tubular epithelial cells. Given the lack of EOC retention within the kidney, we considered whether these cells may be secreting factors that diminish oxidative stress. The accumulation of ROS within NRK

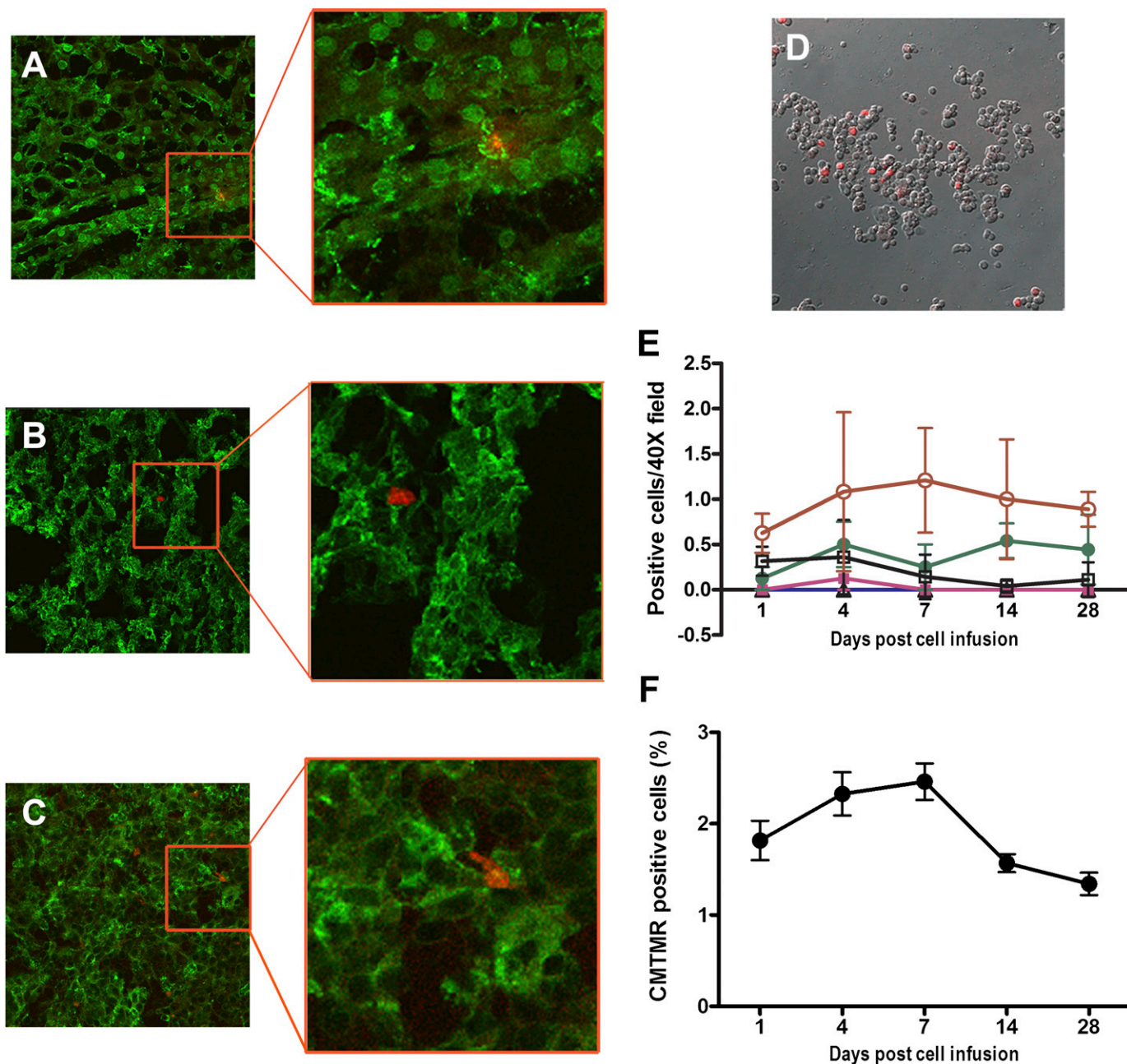


FIG. 5. In vivo tracking of infused EOCs. Abundant CMTMR-labeled EOC-labeled cells were present in the liver (A), spleen (B), lung (C), and bone marrow (D), contrasting with their absence from kidney and heart. Quantification of CMTMR-positive cells shows their persistence in the liver, spleen, lung (E), and bone marrow (F) over the 28-day study period, persisting in all but the latter during the 4 weeks of study. In contrast, EOCs rarely were detected in the kidney or heart. A–D: Representative confocal microscopy images taken 4 days after EOC infusion are shown. Red circles, spleen; green circles, liver; black squares, lung; pink squares, heart; blue triangles, kidney. Original magnification: $\times 40$. $n = 12$ images from three animals per time point. (A high-quality digital representation of this figure is available in the online issue.)

cells, as demonstrated by increased CFDA fluorescence (Fig. 6A and B), increased ninefold when cells were cultured in 25 mmol/L glucose compared with those in 5.6 mmol/L glucose ($P < 0.001$). Coincubation of NRK cells with EOC-conditioned medium from both db/m mice and db/db mice attenuated this high glucose-induced effect ($P < 0.001$).

EOC-conditioned medium inhibits high glucose-induced upregulation of TxnIP in cultured proximal tubular epithelial cells. Given the alterations in renal TxnIP expression with EOC infusion, we next examined whether EOC-derived factors might regulate TxnIP expression in NRK tubular cells that had been cultured in high glucose-containing medium. TxnIP mRNA level was

fivefold higher in cells cultured in 25 mmol/L glucose-containing medium when compared with cells cultured in 5.6 mmol/L glucose. This robust high glucose-associated increase in TxnIP mRNA level was nearly normalized by coincubation with EOC-conditioned medium ($P < 0.05$) (Fig. 6C).

Secreted factors. Given the dearth of labeled EOCs in the kidney, we assessed their secretory activity using a cytokine antibody array (Fig. 7). Among the 40 different cytokines assayed, 11 were detected, several of which were in particularly high abundance, such as interferon γ -induced protein 10 (CXCL10/CRG-2), a chemokine for mesenchymal stem cells (21); interleukin (IL)-1ra (IL-1F3), the endogenous antagonist of the proinflammatory IL-1

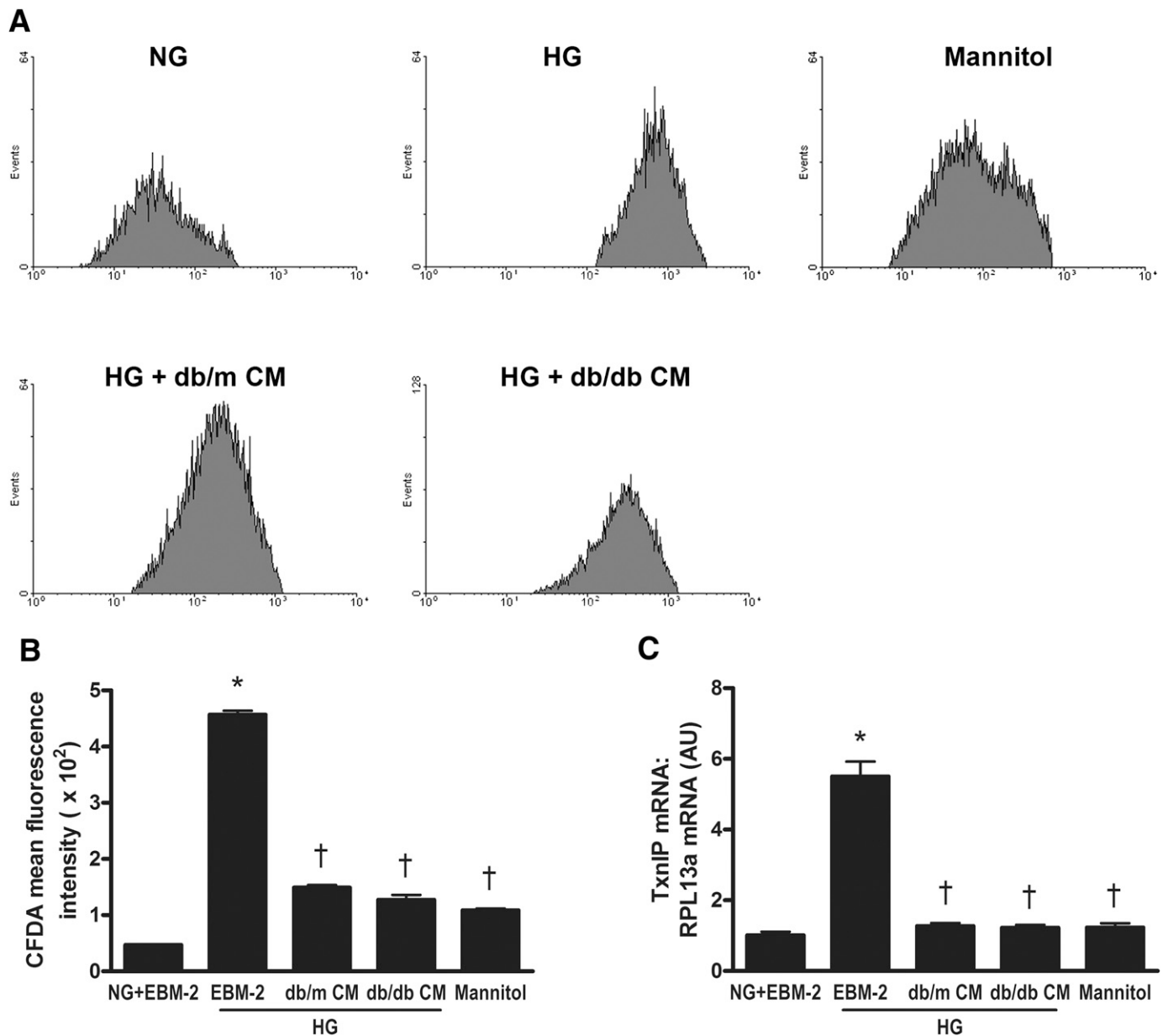
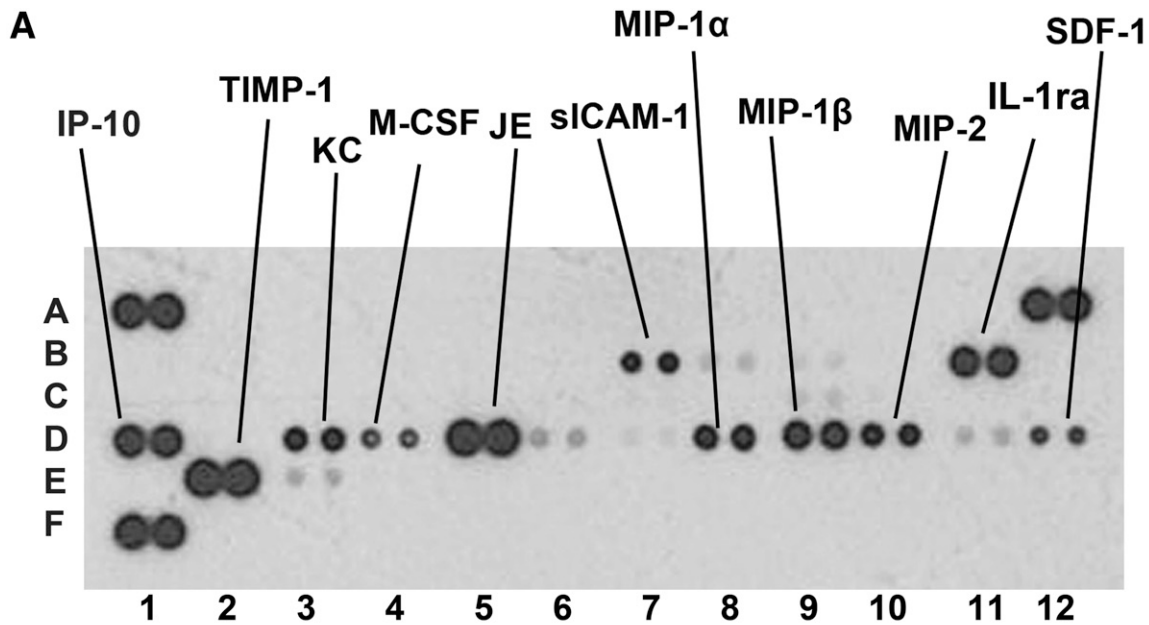


FIG. 6. EOC-conditioned medium reduces glucose-induced ROS and TxnIP overexpression in cultured proximal tubular epithelial cells. **A:** The intracellular ROS production was measured by flow cytometry after staining cells with CM-H2-DCFDA. NRK tubular cells were cultured in normal glucose (NG; 5.6 mmol/L) or high glucose (HG; 25 mmol/L) in the presence of endothelial cell basal medium-2 (EBM-2) or EOC-conditioned medium. A total of 25 mmol/L mannitol served as osmotic control. Both db/m EOC CM and db/db EOC CM attenuated high glucose-induced ROS (**B**) and TxnIP mRNA overexpression (**C**). TxnIP mRNA was expressed relative to the normal glucose group that was arbitrarily assigned a value of 1. Samples were run in triplicate. * $P < 0.001$ vs. normal glucose; † $P < 0.001$ vs. high glucose.



	1	2	3	4	5	6	7	8	9	10	11	12
A	PC	blank	blank	blank	blank	blank	blank	blank	blank	blank	blank	PC
B	BLC	C5a	G-CSF	GM-CSF	I-309	Eotaxin	sICAM-1	IFN- γ	IL-1 α	IL-1 β	IL-1ra	IL-2
C	IL-3	IL-4	IL-5	IL-6	IL-7	IL-10	IL-13	IL-12	IL-16	IL-17	IL-23	IL-27
D	IP-10	I-TAC	KC	M-CSF	JE	MCP-5	MIG	MIP-1 α	MIP-1 β	MIP-2	RANTES	SDF-1
E	TARC	TIMP-1	TNF- α	TREM-1								
F	PC	blank	blank	blank	blank	blank	blank	blank	blank	blank	blank	NC

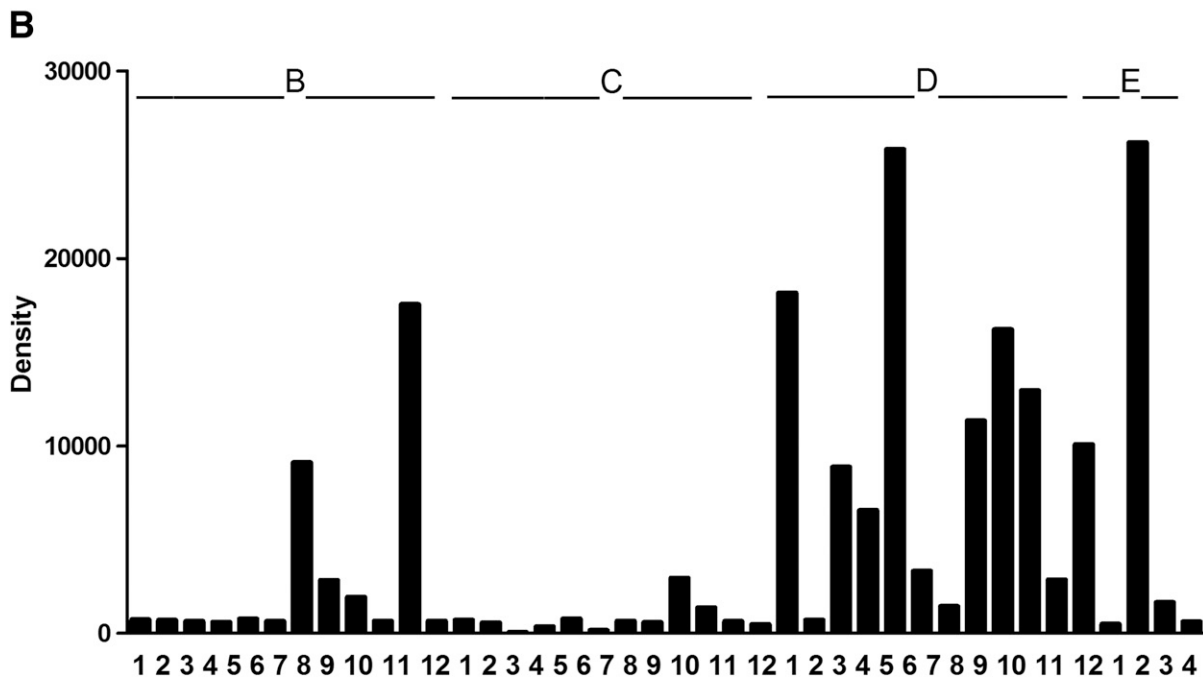


FIG. 7. EOC-secreted factors. EOC-secreted factors were assessed using a cytokine antibody array. Ten cytokines were detected among the 40 different analytes (A) and the magnitude of expression quantified using image analysis (ImageJ; National Institutes of Health) (B). IL-1ra, IL receptor antagonist; IP-10, interferon γ -induced protein 10; JE, also known as MCAF, TDCF, and SMC-CF; KC, keratinocyte-derived chemokine; M-CSF, macrophage colony stimulating factor; MCP-1, monocyte-specific cytokine; MIP-1 α , macrophage inflammatory protein-1 α ; MIP-1 β , macrophage inflammatory protein-1 β ; MIP-2, macrophage inflammatory protein-2; SDF-1, stromal cell-derived factor-1; sICAM-1, soluble intercellular adhesion molecule-1; TIMP-1, tissue inhibitor of metalloproteinase-1.

receptor (22); and tissue inhibitor of metalloproteinase-1, an inhibitor of matrix metalloproteinases with antiapoptotic action (23). Together these factors, among others, indicate the potential for the secretory output of EOCs to mobilize other reparative cell types, dampen inflammation, and protect cells from injury and death.

DISCUSSION

Using a well-established rodent model of diabetic nephropathy, a single infusion of EOCs not only ameliorated oxidative stress but also reduced extracellular matrix deposition and tubular epithelial cell apoptosis. In addition to these structural effects, the progressive rise in albuminuria, characteristic of the db/db mouse model of experimental nephropathy, also was attenuated. Despite these benefits, however, only minimal retention of administered cells was noted in the kidneys of diabetic animals, contrasting with their relative abundance in the liver, spleen, and bone marrow. These findings, in conjunction with the ability of EOC-conditioned medium to abrogate high glucose-induced oxidative stress *in vitro*, suggest that this form of cell therapy may mediate its effects by mechanisms that include, at least in part, the elaboration of soluble factors with antioxidant activity that act at distant sites.

The initial description of circulating bone marrow-derived EOCs by Asahara and colleagues (24,25) more than a decade ago has been followed by a deluge of studies, many using a range of different cell types although still referring to them all as endothelial progenitor cells. To date, however, no unique cell surface marker(s) have been shown to specifically identify the cell types responsible for the reparative activity. Instead, many investigators have used a combination of cell surface markers or alternatively, as in the current study, described them primarily according to the culture techniques used to produce them. With the latter system of classification, adherent bone marrow cells maintained in endothelial media are referred to as either EOCs or late-outgrowth cells, depending on their length of culture, differing with regard to their lineage, phenotypic markers, and function (7,26). Although late-outgrowth cells more closely resemble mature endothelial cells, EOCs are secretory, tend not to integrate into pre-existing structures, and exhibit a phenotype that seems most closely related to immature monocytes (7,27). In accordance with this nomenclature, the cells used in the current study, having been cultured for 7–10 days, would be classified as EOCs. Their cell surface markers, although substantially different from freshly isolated bone marrow cells, expressed markers such as CD34 and VEGFR-2 that have been typically used to define so-called endothelial progenitor cells (28).

The mechanisms by which progenitor cells mediate organ repair and regeneration remain speculative. Although their differentiation into mature parenchymal cells or their fusion with such cells was initially believed to account for their beneficial effects, later studies have emphasized the paracrine actions of bone marrow-derived cells. However, with regard to their effects in the kidney, still other mechanisms may be operational. In particular, several very recent studies have reported the near-complete absence of the administered cells in the kidney, despite notable improvements in organ function and structure. For instance, in ischemic and cisplatin-induced acute kidney injury, three different groups have reported the dearth or

absence of infused marrow stromal cells in the kidney, although renal repair was enhanced in each (3,29,30). Likewise, Yuen et al. (8) recently reported the absence of infused EOCs in the remnant kidney model of chronic renal disease, despite a reduction in proteinuria and improvement in glomerular filtration rate. Although the findings in some of these studies had been interpreted as being the consequence of a paracrine effect that might occur during the cell's brief sojourn through the kidney, other interpretations also are plausible. In particular, using different cell types and in both acute and chronic kidney injury, both Bi et al. (3) and Yuen et al. (8) have provided evidence of an endocrine mechanism to explain the beneficial effects of cell therapy. Consistent with these studies, we also noted the near-total absence of labeled EOCs in the kidneys of diabetic mice, contrasting with their abundance in the liver, lung, spleen, and bone marrow, suggesting that these cells may be exerting their effects by the distant secretion of renoprotective factors.

Hyperglycemia-induced overproduction of superoxide by the mitochondrial electron transport chain provides a unifying and coherent theme for understanding the pathogenesis of diabetes complications (11,31). Molecular species vary in their propensity to oxidative damage. For instance, the sulfur-containing amino acid residues cysteine and methionine are exquisitely sensitive to oxidative stress (32), although they also can be readily reduced by the enzyme, Trx (33). This highly and near-ubiquitously expressed di-thiol protein efficiently reduces oxidized sulfhydryl groups. Its activity, however, is tightly regulated by an endogenous inhibitor, TxnIP, a small 38-amino acid protein (34) that not only impedes the reductive capacity of Trx but also promotes apoptosis (35). Among the factors known to regulate TxnIP expression, the induction of its transcription in response to high glucose, reflecting the carbohydrate response element in its promoter (36), is particularly dramatic and widespread (12–17). As previously reported (16), we also noted increased TxnIP mRNA in the kidneys of diabetic animals. This overexpression was, however, substantially ameliorated in diabetic mice that had received EOCs. Likewise, incubating kidney cells in high glucose resulted in increased TxnIP. However, although still in 25 mmol/L glucose, incubating these same cells in the presence of culture medium that had been used to grow EOCs resulted in normalization of TxnIP mRNA. These findings suggest that the secretory product(s) of EOCs may dampen oxidative stress in the diabetic kidney by abrogating the high glucose-induced upregulation of TxnIP overexpression. Although reduced, the increased ROS in animals that received EOCs was not normalized, possibly reflecting the absence of any demonstrable effect of EOC treatment on *Nox-4* expression.

Diabetic nephropathy is characterized histopathologically by glomerulosclerosis, interstitial fibrosis, and tubular atrophy (37,38). Unfortunately, like all rodent models of diabetes complications, the db/db mouse is imperfect. It does, however, display a range of structural and functional features akin to human disease. For instance, mesangial expansion, a close correlate of kidney dysfunction in patients with diabetic nephropathy (39), is a prominent histopathological feature of db/db mice. In the current study, we found that EOC administration diminished mesangial expansion in diabetic mice, and although the peritubular collagen deposition seen in the db/db mouse is relatively modest, this too was reduced by EOC treatment.

In addition to fibrosis, tubular atrophy also is a feature of disease progression in diabetic nephropathy (37,40). Although the mechanisms responsible for the atrophy are incompletely understood, apoptosis is likely to contribute (37). Like humans (37,41), tubular apoptosis is a feature of diabetic kidney disease in rats and mice (20,42,43), where ROS has been shown to play a key role in its development (44,45). In the current study, tubular epithelial cell apoptosis, recognized by the presence of DNA fragmentation, was increased in the kidneys of db/db mice. EOC administration reduced the extent of TUNEL labeling to that seen in nondiabetic db/m mice, in association with reduction in ROS.

The equally beneficial effects of EOCs derived from diabetic as well as nondiabetic mice, demonstrated in the current study, highlights the potential for autologous therapy in humans. Of note, the cells were administered intravenously and not directly into the kidney parenchyma. Indeed, the beneficial effects were apparent in the absence of their retention within the kidney, a finding that is consistent with the secretory activity of these cells that included the ability to diminish glucose-induced stimulation of TxnIP expression. Whether similar mechanisms apply to other cell types, to other models of diabetic nephropathy, or ultimately to humans, however, remains speculative.

ACKNOWLEDGMENTS

The studies were supported by grants from the Canadian Institutes of Health Research and the Physicians' Services Incorporated Foundation. This research was funded in part by the Canada Research Chair Program. D.A.Y. is sponsored by a KRESCENT postdoctoral fellowship. A.A. is a Canadian Diabetes Association Clinician Scientist. D.K. was sponsored by a Summer Student Award from the Banting and Best Diabetes Centre, University of Toronto. K.A.C. is supported by a Clinician Scientist Award from the Heart and Stroke Foundation of Ontario. R.E.G. is the Canada Research Chair in Diabetes Complications.

No potential conflicts of interest relevant to this article were reported.

Y.Z., D.A.Y., A.A., K.T., S.L.A., D.K., K.A.C., M.G.K., and R.E.G. contributed to the research data. Y.Z., D.A.Y., A.A., K.T., and R.E.G. contributed to the discussion. Y.Z. and R.E.G. wrote the manuscript. Y.Z., D.A.Y., A.A., and R.E.G. reviewed the manuscript. R.E.G. is the guarantor of this work and, as such, had full access to all the data in the study and takes responsibility for the integrity of the data and the accuracy of the data analysis.

Parts of this study were presented in abstract form at the 43rd Annual Meeting and Scientific Exposition of the American Society of Nephrology, Denver, Colorado, 16–21 November 2010.

The authors are greatly appreciative of the excellent animal care provided by Christine Botelho and Bailey Stead (St. Michael's Hospital).

REFERENCES

- Alaiti MA, Ishikawa M, Costa MA. Bone marrow and circulating stem/progenitor cells for regenerative cardiovascular therapy. *Transl Res* 2010; 156:112–129
- Hofmann M, Wollert KC, Meyer GP, et al. Monitoring of bone marrow cell homing into the infarcted human myocardium. *Circulation* 2005;111:2198–2202
- Bi B, Schmitt R, Israilova M, Nishio H, Cantley LG. Stromal cells protect against acute tubular injury via an endocrine effect. *J Am Soc Nephrol* 2007;18:2486–2496
- Gnecchi M, Zhang Z, Ni A, Dzau VJ. Paracrine mechanisms in adult stem cell signaling and therapy. *Circ Res* 2008;103:1204–1219
- Di Santo S, Yang Z, Wyler von Ballmoos M, et al. Novel cell-free strategy for therapeutic angiogenesis: in vitro generated conditioned medium can replace progenitor cell transplantation. *PLoS ONE* 2009;4:e5643
- Kumar AH, Caplice NM. Clinical potential of adult vascular progenitor cells. *Arterioscler Thromb Vasc Biol* 2010;30:1080–1087
- Hur J, Yoon CH, Kim HS, et al. Characterization of two types of endothelial progenitor cells and their different contributions to neovascularization. *Arterioscler Thromb Vasc Biol* 2004;24:288–293
- Yuen DA, Connelly KA, Advani A, et al. Culture-modified bone marrow cells attenuate cardiac and renal injury in a chronic kidney disease rat model via a novel antifibrotic mechanism. *PLoS ONE* 2010;5:e9543
- Yang Z, von Ballmoos MW, Faessler D, et al. Paracrine factors secreted by endothelial progenitor cells prevent oxidative stress-induced apoptosis of mature endothelial cells. *Atherosclerosis* 2010;211:103–109
- Brownlee M. Biochemistry and molecular cell biology of diabetic complications. *Nature* 2001;414:813–820
- Forbes JM, Coughlan MT, Cooper ME. Oxidative stress as a major culprit in kidney disease in diabetes. *Diabetes* 2008;57:1446–1454
- Hirota T, Okano T, Kokame K, Shirota-Ikejima H, Miyata T, Fukada Y. Glucose down-regulates Per1 and Per2 mRNA levels and induces circadian gene expression in cultured Rat-1 fibroblasts. *J Biol Chem* 2002;277:44244–44251
- Kobayashi T, Uehara S, Ikeda T, Itadani H, Kotani H. Vitamin D3 up-regulated protein-1 regulates collagen expression in mesangial cells. *Kidney Int* 2003;64:1632–1642
- Cheng DW, Jiang Y, Shalev A, Kowluru R, Crook ED, Singh LP. An analysis of high glucose and glucosamine-induced gene expression and oxidative stress in renal mesangial cells. *Arch Physiol Biochem* 2006;112:189–218
- Qi W, Chen X, Gilbert RE, et al. High glucose-induced thioredoxin-interacting protein in renal proximal tubule cells is independent of transforming growth factor-beta1. *Am J Pathol* 2007;171:744–754
- Advani A, Gilbert RE, Thai K, et al. Expression, localization, and function of the thioredoxin system in diabetic nephropathy. *J Am Soc Nephrol* 2009; 20:730–741
- Schulze PC, Yoshioka J, Takahashi T, He Z, King GL, Lee RT. Hyperglycemia promotes oxidative stress through inhibition of thioredoxin function by thioredoxin-interacting protein. *J Biol Chem* 2004;279:30369–30374
- Wu LL, Cox A, Roe CJ, Dziadek M, Cooper ME, Gilbert RE. Transforming growth factor β 1 and renal injury following subtotal nephrectomy in the rat: role of the renin-angiotensin system. *Kidney Int* 1997;51:1553–1567
- Advani A, Kelly DJ, Advani SL, et al. Role of VEGF in maintaining renal structure and function under normotensive and hypertensive conditions. *Proc Natl Acad Sci USA* 2007;104:14448–14453
- Zhang Y, Wada J, Hashimoto I, et al. Therapeutic approach for diabetic nephropathy using gene delivery of translocase of inner mitochondrial membrane 44 by reducing mitochondrial superoxide production. *J Am Soc Nephrol* 2006;17:1090–1101
- Kalwitz G, Andreas K, Endres M, et al. Chemokine profile of human serum from whole blood: migratory effects of CXCL-10 and CXCL-11 on human mesenchymal stem cells. *Connect Tissue Res* 2010;51:113–122
- Fearon WF, Fearon DT. Inflammation and cardiovascular disease: role of the interleukin-1 receptor antagonist. *Circulation* 2008;117:2577–2579
- Stetler-Stevenson WG. Tissue inhibitors of metalloproteinases in cell signaling: metalloproteinase-independent biological activities. *Sci Signal* 2008;1:re6
- Asahara T, Masuda H, Takahashi T, et al. Bone marrow origin of endothelial progenitor cells responsible for postnatal vasculogenesis in physiological and pathological neovascularization. *Circ Res* 1999;85:221–228
- Asahara T, Murohara T, Sullivan A, et al. Isolation of putative progenitor endothelial cells for angiogenesis. *Science* 1997;275:964–967
- Yoon CH, Hur J, Park KW, et al. Synergistic neovascularization by mixed transplantation of early endothelial progenitor cells and late outgrowth endothelial cells: the role of angiogenic cytokines and matrix metalloproteinases. *Circulation* 2005;112:1618–1627
- Krenning G, van Luyn MJ, Harmsen MC. Endothelial progenitor cell-based neovascularization: implications for therapy. *Trends Mol Med* 2009;15:180–189
- Yoder MC, Mead LE, Prater D, et al. Redefining endothelial progenitor cells via clonal analysis and hematopoietic stem/progenitor cell principals. *Blood* 2007;109:1801–1809
- Tögel F, Hu Z, Weiss K, Isaac J, Lange C, Westenfelder C. Administered mesenchymal stem cells protect against ischemic acute renal failure through differentiation-independent mechanisms. *Am J Physiol Renal Physiol* 2005;289:F31–F42

30. Duffield JS, Park KM, Hsiao LL, et al. Restoration of tubular epithelial cells during repair of the postischemic kidney occurs independently of bone marrow-derived stem cells. *J Clin Invest* 2005;115:1743–1755
31. Brownlee M. The pathobiology of diabetic complications: a unifying mechanism. *Diabetes* 2005;54:1615–1625
32. Berlett BS, Stadtman ER. Protein oxidation in aging, disease, and oxidative stress. *J Biol Chem* 1997;272:20313–20316
33. Yamawaki H, Berk BC. Thioredoxin: a multifunctional antioxidant enzyme in kidney, heart and vessels. *Curr Opin Nephrol Hypertens* 2005;14:149–153
34. Chen KS, DeLuca HF. Isolation and characterization of a novel cDNA from HL-60 cells treated with 1,25-dihydroxyvitamin D-3. *Biochim Biophys Acta* 1994;1219:26–32
35. Xiang G, Seki T, Schuster MD, et al. Catalytic degradation of vitamin D up-regulated protein 1 mRNA enhances cardiomyocyte survival and prevents left ventricular remodeling after myocardial ischemia. *J Biol Chem* 2005;280:39394–39402
36. Minn AH, Hafele C, Shalev A. Thioredoxin-interacting protein is stimulated by glucose through a carbohydrate response element and induces beta-cell apoptosis. *Endocrinology* 2005;146:2397–2405
37. Verzola D, Gandolfo MT, Ferrario F, et al. Apoptosis in the kidneys of patients with type II diabetic nephropathy. *Kidney Int* 2007;72:1262–1272
38. Gilbert RE, Cooper ME. The tubulointerstitium in progressive diabetic kidney disease: more than an aftermath of glomerular injury? *Kidney Int* 1999;56:1627–1637
39. Mauer SM, Steffes MW, Ellis EN, Sutherland DE, Brown DM, Goetz FC. Structural-functional relationships in diabetic nephropathy. *J Clin Invest* 1984;74:1143–1155
40. Bohle A, Mackensen-Haen S, Wehrmann M. Significance of postglomerular capillaries in the pathogenesis of chronic renal failure. *Kidney Blood Press Res* 1996;19:191–195
41. Kumar D, Zimpelmann J, Robertson S, Burns KD. Tubular and interstitial cell apoptosis in the streptozotocin-diabetic rat kidney. *Nephron, Exp Nephrol* 2004;96:e77–e88
42. Kelly DJ, Cox AJ, Tolcos M, Cooper ME, Wilkinson-Berka JL, Gilbert RE. Attenuation of tubular apoptosis by blockade of the renin-angiotensin system in diabetic Ren-2 rats. *Kidney Int* 2002;61:31–39
43. Zhang W, Khanna P, Chan LL, Campbell G, Ansari NH. Diabetes-induced apoptosis in rat kidney. *Biochem Mol Med* 1997;61:58–62
44. Bagby SP. Diabetic nephropathy and proximal tubule ROS: challenging our glomerulocentricity. *Kidney Int* 2007;71:1199–1202
45. Brezniceanu ML, Lau CJ, Godin N, et al. Reactive oxygen species promote caspase-12 expression and tubular apoptosis in diabetic nephropathy. *J Am Soc Nephrol* 2010;21:943–954